



# CHALMERS

## Chalmers Publication Library

### **Improving the Calibration Efficiency of an Array Fed Reflector Antenna through Con-strained Beamforming**

This document has been downloaded from Chalmers Publication Library (CPL). It is the author's version of a work that was accepted for publication in:

**IEEE Transactions on Antennas and Propagation (ISSN: 0018-926X)**

Citation for the published paper:

Young, A. ; Maaskant, R. ; Ivashina, M. (2014) "Improving the Calibration Efficiency of an Array Fed Reflector Antenna through Con-strained Beamforming". IEEE Transactions on Antennas and Propagation, vol. 61(7), pp. 3538 - 3545.

<http://dx.doi.org/10.1109/TAP.2013.2255577>

Downloaded from: <http://publications.lib.chalmers.se/publication/202944>

Notice: Changes introduced as a result of publishing processes such as copy-editing and formatting may not be reflected in this document. For a definitive version of this work, please refer to the published source. Please note that access to the published version might require a subscription.

Chalmers Publication Library (CPL) offers the possibility of retrieving research publications produced at Chalmers University of Technology. It covers all types of publications: articles, dissertations, licentiate theses, masters theses, conference papers, reports etc. Since 2006 it is the official tool for Chalmers official publication statistics. To ensure that Chalmers research results are disseminated as widely as possible, an Open Access Policy has been adopted. The CPL service is administrated and maintained by Chalmers Library.

(article starts on next page)

# Improving the Calibration Efficiency of an Array Fed Reflector Antenna through Constrained Beamforming

André Young, Marianna V. Ivashina, *Member, IEEE*, Rob Maaskant, *Member, IEEE*, Oleg A. Iupikov, and David B. Davidson, *Fellow, IEEE*

**Abstract**—Calibrating for the radiation pattern of a multi-beam Phased Array Feed (PAF) based radio telescope largely depends on the accuracy of the pattern model, and the availability of suitable reference sources to solve for the unknown parameters in the pattern model. It is shown how the efficiency of this pattern calibration for PAF antennas can be improved by conforming the beamformed far field patterns to a two-parameter physics-based analytic reference model through the use of a Linearly Constrained Minimum Variance (LCMV) beamformer. Through this approach, which requires only a few calibration measurements, an accurate and simple pattern model is obtained. The effects of the model parameters on the directivity and sidelobe levels of multiple scanned beams are investigated, and these results are used in an example PAF beamformer design for the proposed MeerKAT antenna. Compared to a typically used Maximum Directivity (*MaxDir*) beamformer, the proposed constrained beamforming method is able to produce beam patterns over a wide Field-of-View (*FoV*) that are modeled with a higher degree of accuracy and result in a significant reduction in pattern calibration complexity.

**Index Terms**—Antenna Radiation Patterns, Array Signal Processing, Calibration, Phased Array Feeds, Radio Astronomy.

## I. INTRODUCTION

CALIBRATION of radio telescopes requires accurate models of the instrumental parameters and propagation conditions that affect the reception of radio waves [1]. These effects vary over time and the model parameters have to be determined at the time of observation through a number of calibration measurements. Furthermore, the calibration measurements should complete in a relatively short time and may be repeated often over the course of an observation during which the instrumental and atmospheric conditions can change significantly. One of the instrumental parameters that needs accurate characterization is the radiation pattern of the antenna,

which is especially challenging in the arena of future array based multiple beam radio telescopes [2]–[4], both due to the complexity of these instruments, as well as the increased size of the Field-of-View (*FoV*). Above the requirement that the radiation pattern should be accurately known, currently developed techniques for the pattern calibration of these devices also emphasize the need for beams<sup>1</sup> over the *FoV* that are similar in shape, and that each beam varies smoothly with time, frequency, and over the main beam angular region [5]. Such beams can be described by simpler models, which reduce the number of pattern model parameters that need to be solved for, and also simplify the complexity of direction dependent calibration which is vitally important for future radio telescopes [6]–[10]. However, achieving patterns exhibiting these qualities, while also meeting the already stringent sensitivity requirements, presents a difficult task.

Previously, beamforming techniques have been used to create similarly shaped beams over the *FoV* by conforming them to an elliptical reference pattern, but at the cost of a significant loss in sensitivity [6] (up to 25%). An initial study has shown that this loss can be reduced by applying the same beamforming technique, but using a reference pattern that more closely matches the natural radiation characteristics of large aperture antennas [11]. Therein, the first term of the Jacobi-Bessel (*JB*) series solution of reflector antenna far field patterns [12], [13] was used as a reference pattern to define directional constraints in a Linearly Constrained Minimum Variance (*LCMV*) beamforming Phased Array Feed (*PAF*). It was found that this first *JB*-term is sufficient to model the patterns of a prime focus single reflector antenna over a wide *FoV* of up to 5 beamwidths, over which the sensitivity reduction was less than 10%. However, when considering a larger scan range, phase aberration effects cause deformation of the radiation patterns to such an extent that this beam model is no longer accurate. Furthermore, when applying this model to an offset reflector antenna for which the asymmetric geometry exacerbates the deformation of scanned patterns [14, *cf.* Figs. 1 and 3], the inclusion of more physics-based information is necessary.

Here, the reference pattern of [11] is extended to model the widening of the scanned beam as well as the change in the phase distribution for an offset dual-reflector antenna

Manuscript received Month 01, 2012; revised Month 01, 2012. This work was supported in part by the Swedish SIDA and VR grants. A. Young and D. B. Davidson acknowledge the support of SKA South Africa and the South African Research Chairs Initiative of the Department of Science and Technology (DST) and National Research Foundation (NRF). Any opinion, findings and conclusions or recommendations expressed in this material are those of the authors and therefore the NRF and DST do not accept any liability with regard thereto.

A. Young and D. B. Davidson are with the Department of Electrical and Electronic Engineering, University of Stellenbosch, Stellenbosch, South Africa, e-mail: ayoung@sun.ac.za, davidson@sun.ac.za

R. Maaskant, M. V. Ivashina, and O. A. Iupikov are with the Department of Signals and Systems, Chalmers University of Technology, Gothenburg, Sweden, email: marianna.ivashina@chalmers.se, rob.maaskant@chalmers.se, oleg.iupikov@chalmers.se

<sup>1</sup>Often referred to as the *direction-dependent gain* or *primary beam* in the radio interferometer community.

by introducing two additional model parameters. It will be shown that this model allows for the accurate characterization of multiple beams over a wide FoV without the need to perform additional calibration measurements. The effects of the model parameters on the directivity and sidelobe levels are investigated for a proposed design of the MeerKAT radio telescope reflector antenna [15]. An LCMV beamformer is designed based on the results of this study, and its performance evaluated through comparison with a Maximum Directivity (*MaxDir*) beamformer.

## II. ANTENNA PATTERN MODEL

The reference pattern employed in [11] to constrain the main beam shape of a scanned reflector is based on the JB-series solution for modeling reflector antenna far field patterns. The first term in this series is the near-boresight approximation of the co-polarized far field pattern radiated by a circular aperture with a uniform amplitude and phase distribution [16], i.e.,

$$F_A(\theta, \phi) \propto \frac{J_1(ka \sin \theta)}{ka \sin \theta} \equiv \text{jinc}(ka \sin \theta) \quad (1)$$

where  $a$  is the aperture radius,  $k$  is the free space wavenumber, and  $J_1$  is the Bessel function of the first kind of order one. Patterns radiated by more general aperture field distributions, including off-axis patterns of a scanned reflector are represented as a sum of (possibly) many more JB-terms. However, the first term in the series is still dominant over an angular region around the beam maximum. To obtain a pattern function that applies to more general aperture field distributions, certain modifications to the reference pattern (1) are required as detailed below.

In order to control the beamwidth of the pattern model, an angular scaling parameter  $s$  is introduced by letting  $a \rightarrow sa$ , which enables accounting for widening of the beam due to under-illumination of the reflector aperture or coma aberration when scanning [17], [18]<sup>2</sup>. In this sense a distinction can be made between the *physical* aperture radius  $a$ , and an *effective* aperture radius  $sa$ , where  $s \lesssim 1$ .

Another limitation of (1) is that it assumes a constant phase distribution of the beam pattern. This implies that the phase reference of the pattern coincides with the phase center of the antenna, defined here for a small angular region of the far field around the main beam center. Whereas this condition is easily satisfied for an on-axis beam of a prime focus reflector, the proper choice for the phase reference is not straightforward for scanned beams. In the latter case it is more convenient to keep the phase reference fixed at the center of the projected aperture and to account for a phase variation over the main beam through multiplying the pattern model by

$$F_\psi(\theta, \phi) = \exp(j\Psi \sin \theta \cos(\phi - \phi_0)) \quad (2)$$

in which  $\Psi$  is a constant that determines the phase gradient, and  $\phi_0$  defines the direction of the phase center shift. The value of  $\phi_0$  can be determined by noting that for a scanned beam

<sup>2</sup>The pattern deformations for off-axis scanning are known to be asymmetrical, and since the analytic model is used here to constrain the pattern shape so that it is easily modeled, we elect to use a circularly symmetric pattern model.

the phase center shift is in the scan plane. It can be shown that the value of  $\Psi$  is proportional to the phase center shift projected orthogonally to the direction of observation [19].

Combining (1) and (2) gives the extended reference pattern model<sup>3</sup>

$$F(s, \Psi; \theta, \phi) = \text{jinc}(ksa \sin \theta) e^{j\Psi \sin \theta \cos(\phi - \phi_0)} \quad (3)$$

in which the the amplitude and phase distributions of the reference pattern are controlled independently by the parameters  $s$  and  $\Psi$ , respectively. Note that (3) will serve as a *reference pattern* for deriving the directional constraints in an LCMV beamformer, as well as a pattern *calibration model* to describe the realized beamformed pattern.

## III. BEAMFORMING STRATEGY

An LCMV beamformer is implemented which minimizes the power received by the antenna due to noise subject to linear constraints that conform the co-polarized pattern shape to the reference pattern in (3). The beamformer weights applied to the elements of the PAF are calculated according to [20] [21, p. 526]

$$\mathbf{w}_{\text{LCMV}}^H = \mathbf{g}^H [\mathbf{G}^H \mathbf{C}^{-1} \mathbf{G}]^{-1} \mathbf{G}^H \mathbf{C}^{-1} \quad (4)$$

in which  $\mathbf{x}^H$  means the complex conjugate transpose of  $\mathbf{x}$ ,  $\mathbf{C}$  is the noise covariance matrix,  $\mathbf{g}$  is the constraints vector, and  $\mathbf{G}$  is the directional constraint matrix. For  $L$  elements in the array and constraints enforced in the  $K$  different directions  $\{\Omega_1, \Omega_2, \dots, \Omega_K\}$ ,  $\mathbf{G}$  is an  $L \times K$  matrix in which the  $i$ th column contains the signal response vector of the array due to a plane wave incident from direction  $\Omega_i$ , and the corresponding element  $g_i$  in the vector  $\mathbf{g}$  is the constraint value enforced on the pattern in that direction. The choice of these constraint parameters is discussed in the following subsections.

In this study the performance of the LCMV beamformer is compared to that for the standard MaxSNR beamformer (no directional constraints). In this case the beamformer weights are calculated according to [22] [21, p. 450]

$$\mathbf{w}_{\text{MaxSNR}} = \mathbf{C}^{-1} \mathbf{v} \quad (5)$$

where  $\mathbf{v}$  is the signal response vector of the array due to a plane wave incident from the direction of interest. In this study a noiseless system is assumed which means that the noise correlation matrix  $\mathbf{C}$  can be taken equal to the identity matrix, and therefore the weights in (5) maximize the received signal power. It can be shown that this is approximately equivalent to maximizing the directivity, if the antenna exhibits low loss and low scattering, as is the case for the PAF used herein. Therefore the beamformer using the weights in (5) shall hereafter be referred to as a *MaxDir* (Maximum Directivity) beamformer.

<sup>3</sup>Henceforth we assume that  $(\theta, \phi)$  are defined in a local coordinate system for each beam in which the maximum is at  $\theta = 0$ .

### A. Number of Constraints and Pattern Calibration Measurements

Each of the weights applied to the PAF elements presents a complex Degree of Freedom (*DoF*) available for optimizing the beamformed pattern, and for each constraint enforced on the pattern shape the number of *DoFs* available to maximize the directivity is reduced. The implication of this is that constraints should be selected carefully to obtain the desired pattern shape while retaining enough freedom in the system to achieve a sufficiently high directivity.

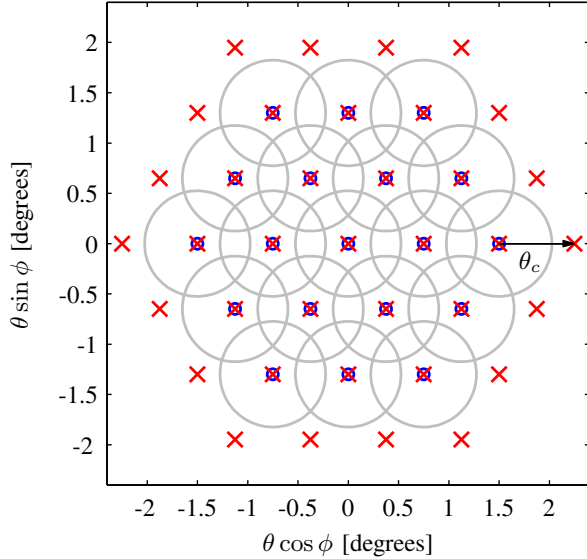


Fig. 1. Beams arranged over the FoV to enable reuse of constraint directions between adjacent beams. Nominal half-power contours (HPBW =  $1^\circ$ ) and constraint positions of each beam shown as solid lines and crosses, respectively.

Furthermore, the number of constraints has an impact on the calibration efficiency because a pattern calibration measurement is required for each constraint direction to determine the signal response vector of the PAF [22]. Since these measurements can become time consuming, we need to minimize the number of constraint directions to ensure that the system parameters do not drift significantly during this procedure. It is worth pointing out that since both the amplitude and phase of the signal response vectors are needed, this may require the use of an auxiliary antenna to recover the phase information in addition to a natural celestial calibration source [23].

### B. Constraint Positions

We aim to conform the beam to the reference pattern down to a certain level below the beam maximum, so we choose to position the constraints within the corresponding angular region. Also, the total required number of pattern calibration measurements may be reduced by positioning the constraint directions at the centers of adjacent beams, as shown in Fig. 1. This allows the reuse of measurement data between multiple beams which is readily available in this type of measurement. In this example six constraints are enforced in a circularly symmetric fashion around, and an angular distance

$\theta_c$  from the beam center for each beam. This arrangement results in a fine enough sampling of the FoV since the half-power beams overlap [22], and the constraints are enforced around the -8 to -5 dB level. In this case only 37 pattern calibration measurements are needed to realize a total of 19 constrained beams over the FoV, which is a minor increase over that for unconstrained beamforming as in (5). The 18 additional measurements are necessary for the constraints enforced around the edge of the FoV.

### C. Constraints Vector

The constraints vector  $\mathbf{g}$  in (4) is formed by evaluating the reference pattern in (3) at the beam center and the directions of constraints  $\Omega_i = \{\theta_c, \phi_i\}$ , i.e.,

$$g_i = \begin{cases} F(s, \Psi; 0, 0) & \text{for } i = 1 \\ F(s, \Psi; \theta_c, \phi_i) & \text{for } i = 2, 3, \dots, 7, \end{cases} \quad (6)$$

where the selection of the model parameters  $s$  and  $\Psi$  has to be made for each scan direction to account for the beam widening and the increasing phase gradient over the main lobe region. In order not to compromise the beam sensitivity too much, it is natural to derive the initial physics-based values  $s = s_0$  and  $\Psi = \Psi_0$  from the reference patterns realized by the MaxDir beamformer, i.e.,

$$s_0 = \frac{a_{\text{eff,MaxDir}}}{a} = \frac{\lambda \sqrt{D_{\text{MaxDir}}}}{2\pi a} \quad (7a)$$

$$\Psi_0 = \left. \frac{\partial \psi_{\text{MaxDir}}}{\partial \theta} \right|_{\theta=0, \phi=\phi_0} \quad (7b)$$

where  $a_{\text{eff,MaxDir}}$  is the effective aperture radius, and  $D_{\text{MaxDir}}$  and  $\psi_{\text{MaxDir}}$  are the directivity and phase pattern over the main lobe region, respectively, of the MaxDir beam. Using thus obtained values for the parameters  $s$  and  $\Psi$  result in rotationally symmetric beams that have sensitivities close to the MaxDir beams. However, this choice leads to a sidelobe level (*SLL*) that can be relatively high for certain (off-axis) beams. Hence, the optimum values for  $s$  and  $\Psi$  may be slightly different from  $s_0$  and  $\Psi_0$  depending upon the required antenna beam performance, such as minimum beam sensitivity and maximum allowable *SLL*, as explained below for a numerical example.

## IV. NUMERICAL RESULTS

In this section we investigate the trade-off effects of the beam model parameters  $s$  and  $\Psi$  on the directivity and *SLL*. After choosing  $s$  and  $\Psi$ , the beam model accuracy is examined as the difference between the resulting LCMV-beamformed pattern and the reference beam. As a numerical example, we present results for an offset Gregorian geometry based on the MeerKAT radio telescope reflector antenna [15] by employing simulated primary far-field patterns of the APERTIF PAF [6]. The reflector has a projected diameter of 13.5 m ( $64\lambda$  at 1.42 GHz) and an equivalent focal length to diameter ratio ( $F/D$ ) of 0.55. The APERTIF PAF is a dual-polarized array composed of 121 tapered slot antenna elements. Here all elements in the array (both polarizations) are employed to produce patterns on the sky for each nominal polarization (as

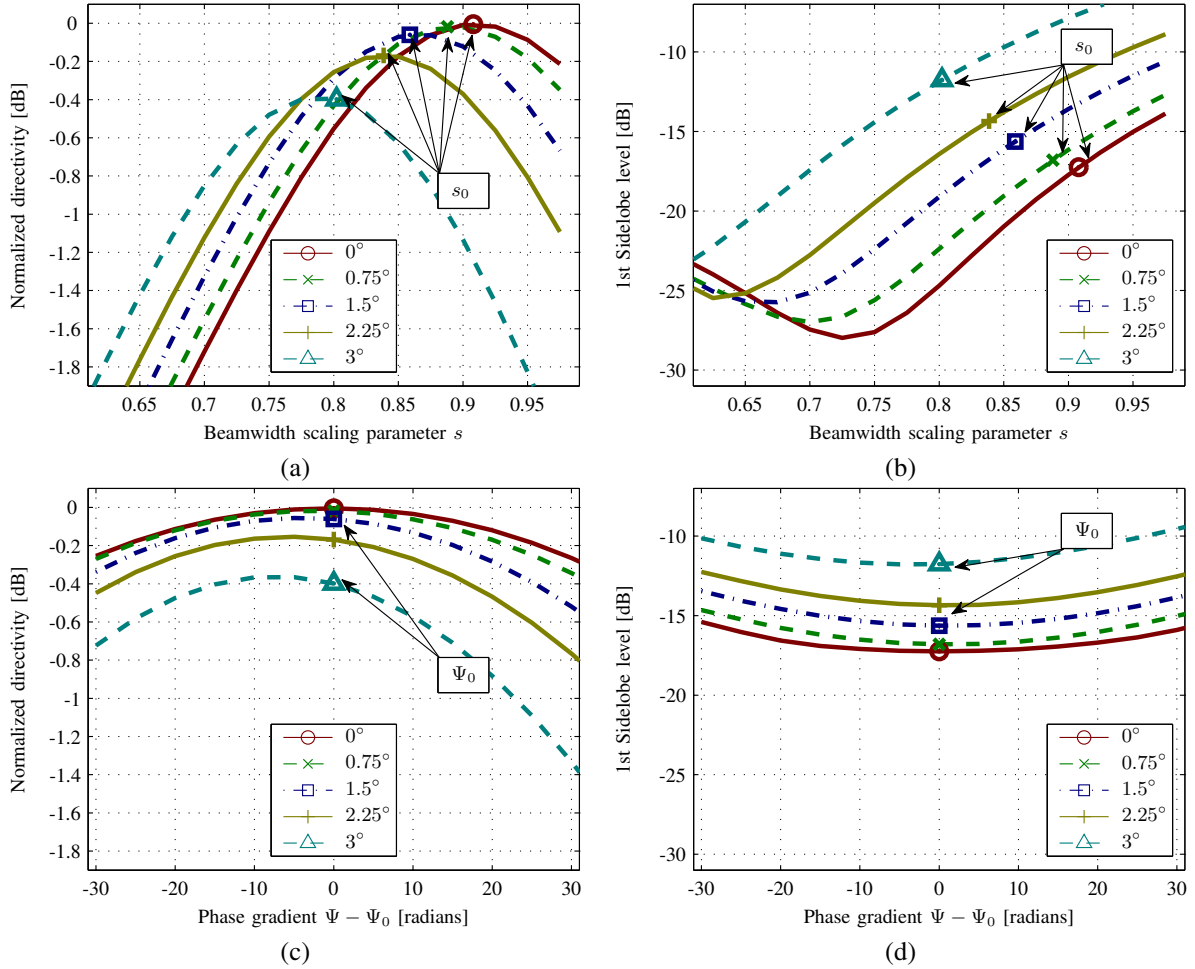


Fig. 2. Effect of model parameters on beam pattern performance. (a) and (c) show the directivity of scanned LCMV patterns relative to that of the on-axis MaxDir pattern for various values of  $s$  and  $\Psi$ , respectively; (b) and (d) show the highest SLL of scanned LCMV patterns for various values of  $s$  and  $\Psi$ , respectively. Markers indicate the results for  $s = s_0$  and  $\Psi = \Psi_0$  for each scan direction.

opposed to a bi-scalar beamformer wherein only elements of one polarization are used, *cf.* [24]). Results presented here are for only one nominal polarization, as the results for either polarization are very similar. The numerical results are shown for the operating frequency of 1.42 GHz at which the half-power beamwidth (HPBW) is approximately  $1^\circ$ , and results were obtained using a toolbox interface [22] to the GRASP software.

#### A. Beam Directivity and Side Lobe Levels

Fig. 2(a) shows the directivity of the LCMV-scanned patterns relative to the corresponding MaxDir patterns as a function of  $s$  (with  $\Psi = \Psi_0$ ) over a scan range of 3 beamwidths in the symmetry plane<sup>4</sup>. Markers indicate the results for the initial values  $s = s_0$  that were derived from the MaxDir beams. As expected, the highest directivity is achieved if  $s$  is close to  $s_0$ , except for far off-axis patterns where it occurs for slightly smaller values of  $s$ . This is attributed to the fact that the computation of  $s_0$  is based solely on the directivity of the MaxDir elliptically-shaped pattern, while  $s_0$  is applied to

<sup>4</sup>Although results are only shown for scanning in a single plane, the conclusions are valid for scanning in all  $\phi$ -directions.

rotationally symmetric patterns pertaining to the same effective aperture size. It is also observed that when choosing  $s = s_0$ , the loss incurred by constrained beamforming is relatively small ( $< 0.4$  dB) over the entire FoV. Letting  $s \rightarrow 1$  results in the edge illumination taper approaching 0 dB as the primary (feed) pattern widens, and a subsequent decrease in directivity due to increasing spillover loss.

The effect of  $s$  on the 1st SLL performance of the LCMV patterns is shown in Fig. 2(b). As one can see, the choice of  $s = s_0$  leads to a significant variation of the SLLs of the scanned beams where the minimum (for the on-axis direction) and maximum (for a scan angle of 3 beamwidths) are around  $-17$  dB and  $-12$  dB, respectively. Decreasing the value of  $s$  improves the SLL, albeit at a moderate cost of a reduction in directivity. This is in accordance with the familiar trade-off between directivity and SLL for reflector antennas. The 2nd SLL is affected similarly to the 1st SLL when  $s$  is varied, and these results are therefore not shown.

The effects of  $\Psi$  on the relative directivity and SLL of the LCMV beamformed patterns were also investigated and the results are shown in Figs. 2(c) and (d). In these figures, the abscissae represent the difference  $\Psi - \Psi_0$  calculated for each scan direction. Over the FoV, the value of  $\Psi_0$  decreases

monotonically from 0 rad for the on-axis pattern to  $-33$  rad for the farthest off-axis scanned pattern, indicating a steady shift of the antenna phase center from the phase reference point. Choosing  $\Psi$  close to  $\Psi_0$  – as opposed to setting it to zero, thereby effectively reducing the pattern model to (1) – resulted in a significant improvement in directivity of far off-axis scanned patterns. This underlines the importance of using a proper reference pattern function such as (3) which represents a more accurate description of the (off-axis) radiation characteristics of the antenna. The effect of small variations of  $\Psi$  around the value  $\Psi_0$  on the relative directivity and SLLs was found to be less pronounced than the effect of parameter  $s$ , so that, generally, the choice  $\Psi = \Psi_0$  yielded the best results.

### B. Calibration Performance

A deviation of the actual beam shape from the one predicted through calibration measurements sets constraints on the dynamic range of the mosaicked images. Although the relationship between the desired dynamic range and pattern calibration error is very complex (and typically requires the analysis of the error propagation effects in the image plane [25], [26]), the required accuracy of the pattern model can be approximately derived from the required image fidelity [27] which is limited by the maximum error present in the beam model. In this section we will therefore use the maximum normalized error in the complex voltage pattern within the 10 dB region when approximating realized beam patterns with (3) as a measure of beamshape calibratability.

The effect of  $s$  on the calibratability of LCMV beamformed patterns is shown in Fig. 3(a). Using the MaxDir equivalent value  $s = s_0$  the maximum error ranges from 0.7 % for on-axis up to 4 % for the widest scan angle. Decreasing the parameter over the range  $s \lesssim s_0$  is seen to slowly increase the model error, whereas increasing  $s > s_0$  is seen to have a more dramatic effect on the model accuracy for wider scan directions due to the increase of the 1st SLL above the 10 dB level. In Fig. 3(b) the effect of  $\Psi$  on the calibratability is shown and for this figure of merit the optimal choice for the phase gradient is as before  $\Psi = \Psi_0$ .

Since the constrained beamformer ensures that the realized beam conforms exactly to (3) at the constraint positions the model error is smallest in the vicinity of these points and the placement of constraints may be optimized to minimize this error within a certain angular region. The effect of  $\theta_c$  on the pattern calibratability is shown in Fig. 3(c). Markers indicate the power level relative to pattern maximum that correspond to the values of  $\theta_c$ . The optimal placement of constraints is seen to be around the  $-5$  dB to  $-7$  dB level.

Furthermore, to examine how the technique performs over a range of frequencies we repeated the above described analysis at several frequencies within the antenna array operation band from 1 to 1.75 GHz. In this study, frequency-dependent parameters were scaled for each of these frequencies (scan directions, positions of constraints for LCMV beamforming, etc.). The results obtained have shown that at the lower frequencies the FoV is limited by the size of the array (that

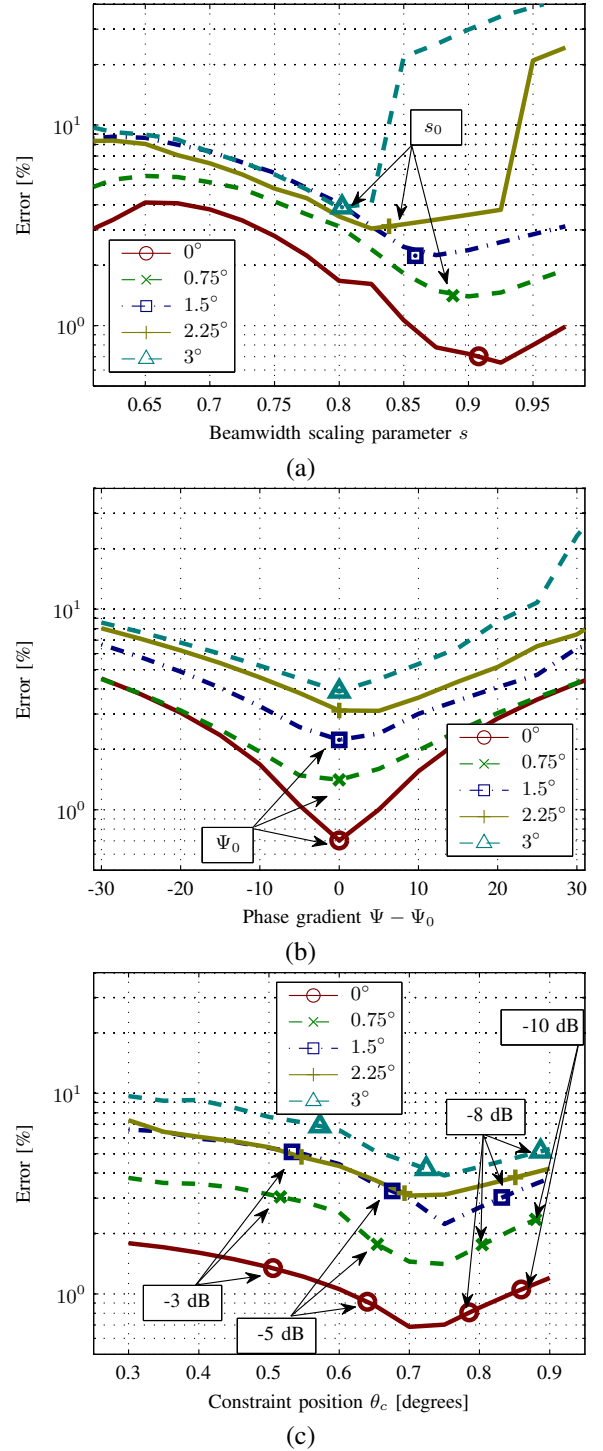


Fig. 3. Maximum normalized error over the 10 dB beamwidth of the LCMV beamformed patterns when approximated by the analytical function (3), and using the same parameter values as was used to define directional constraints. The error is shown as a function of the parameter (a)  $s$ , (b)  $\Psi - \Psi_0$ , and (c)  $\theta_c$ . Default values for these parameters are  $s = s_0$ ,  $\Psi = \Psi_0$ , and  $\theta_c = 0.75^\circ$ .

is the case for any type of the PAF beamformers), although the results for the on-axis and closer scanned directions are similar to those at 1.42 GHz. Hence, the advantages of using the proposed LCMV-based beamforming are also applicable at lower frequencies over a relatively smaller FoV. For higher frequencies, the results for all scan directions (within the FoV of

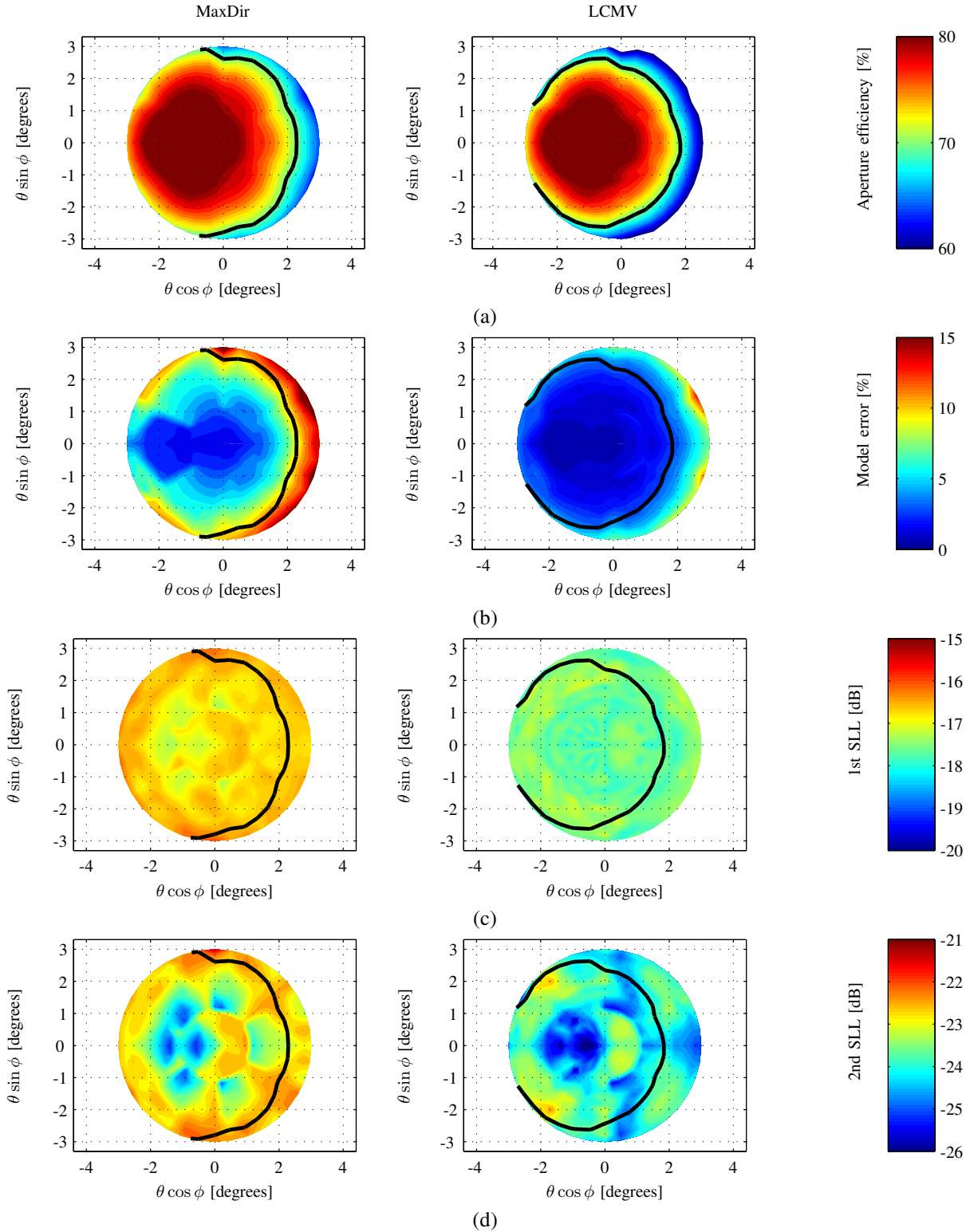


Fig. 4. Comparison of LCMV and MaxDir beamformers over a  $\theta < 3^\circ$  angular region based on (a) aperture efficiency, (b) maximum beam model error, (c) 1st SLL, and (d) 2nd SLL. Figures of merit are shown as functions of beam steering direction over the FoV. Solid lines on all plots indicate the FoV within which aperture efficiency is above 70% for each beamformer. The asymmetry in the results is due to the offset geometry of the antenna.

$\pm 3$  beamwidths) are very similar to those at 1.42 GHz. Based on these observations, we can conclude that the proposed beamforming technique ensures the smooth characteristics of the resulting FoV calibration over a wide frequency band, and does not require additional constraints due to frequency

variation.

### C. Comparison of MaxDir and LCMV beamformers

Using the results from Section IV-A, an LCMV beamformer was implemented to produce a number of beams over a dense

grid within an angular region  $\theta < 3^\circ$ . For each LCMV beam the value of  $s$  was chosen such that the 1st SLL is below -17 dB, and  $\Psi = \Psi_0$  as calculated from a MaxDir beam towards the same scan direction. The performance of the MaxDir and LCMV produced beams were then compared for every scan direction within the angular region of interest.

In Fig. 4(a) the aperture efficiencies achieved with the respective beamformers are shown as a function of scan direction. The asymmetry of the results over the FoV is a consequence of the offset geometry and wide scanning towards  $\phi = 0^\circ$  is seen to result in the largest reduction in efficiency. A FoV was defined for each beamformer as the region within which the aperture efficiency is greater than 70%, the size of which was 23.6 and 19.3 square degrees for the MaxDir and LCMV beamformers, respectively. The boundary of each FoV is indicated on the plots in Fig. 4 as a solid black line, and the results presented below were calculated within the respective regions for the two beamformers.

The beamformers were compared by considering the maximum pattern calibration model error for each of the defined beams over the FoV, which is shown in Fig. 4(b). For the MaxDir beamformer this error ranges from 1.6% up to 10.4%, whereas for the LCMV beamformer the same error ranges from 0.5% up to 4.3% and presents a considerable improvement in accuracy. One prominent factor contributing to the relatively large model error for MaxDir beams, especially at wider scan angles, is the asymmetry of these patterns. As a comparison, the aspect ratio of the half-power contours of the MaxDir beams may be as high as 1.15:1, whereas for the LCMV beams this ratio is less than 1.01:1 for all scan directions. The symmetry of constrained beams therefore also present a significant advantage in terms of reducing the complexity of direction-dependent calibration [6].

Finally, the maximum 1st and 2nd SLLs are shown as a function of scan direction in Figs. 4(c) and (d), respectively. Compared to the MaxDir beams, the LCMV beams have 1st SLLs that are 0.8 dB lower and 2nd SLLs that are 1.0 dB lower, on average over the FoV. The 2nd SLL is of particular interest in the case of MeerKAT, for which the maximum is specified as -23 dB (L-band). The LCMV beamformer meets this specification over most of the FoV (except for wide scanning in the  $\phi \approx 135^\circ, 225^\circ$  directions), whereas the MaxDir beams exceed this limit over a much larger region. In order to quantify the trade-off in sensitivity for this reduction in sidelobes through constrained beamforming, LCMV beams were also realized to yield 1st SLLs within 0.2 dB of that for the MaxDir beams. Following this approach the size of the FoV could be increased by 4.6% to 20.2 square degrees.

## V. CONCLUSIONS AND RECOMMENDATIONS

A constrained beamforming technique that conforms multiple patterns on the sky to a physics-based analytic far field function was presented as a method to improve the calibration efficiency of an array fed reflector antenna. The effects of the two parameters in the analytic model on the pattern performance were investigated, and a procedure by which these parameters could be optimized was proposed. This beamforming approach was shown to have several performance

benefits including circularly symmetric scanned beams over a wide FoV, even for non-symmetric reflector antennas. For the example of the MeerKAT offset Gregorian antenna, this strategy resulted in multiple beams with aperture efficiency above 70% that could be approximated down to the 10 dB level as a single analytic function with an error of less than 5%. In comparison with a conventional MaxDir beamformer, this would reduce the average pattern calibration model error by more than 50%. Finally, the proposed beamforming strategy was found to be effective across a wide frequency band by simply scaling all frequency dependent parameters.

Future work will include the assessment of the proposed beamforming in the presence of external and internal noise sources, as well as experimental demonstration for a practical system.

## REFERENCES

- [1] O. M. Smirnov, "Revisiting the radio interferometer measurement equation. II. Calibration and direction-dependent effects," *Astronomy & Astrophysics*, vol. 527, p. A107, 2011.
- [2] S. Ellingson, T. Clarke, A. Cohen, J. Craig, N. Kassim, Y. Pihlstrom, L. Rickard, and G. Taylor, "The long wavelength array," *Proc. IEEE*, vol. 97, no. 8, pp. 1421–1430, Aug. 2009.
- [3] M. De Vos, A. Gunst, and R. Nijboer, "The lofar telescope: System architecture and signal processing," *Proc. IEEE*, vol. 97, no. 8, pp. 1431–1437, Aug. 2009.
- [4] The Square Kilometre Array. [Online]. Available: <http://www.skatelescope.org>
- [5] O. M. Smirnov, B. S. Frank, I. P. Theron, and I. Heywood, "Understanding the impact of beamshapes on radio interferometer imaging performance," in *Proc. Int. Conf. on Electromagn. in Adv. Applicat. (ICEAA)*, Sep. 2012, pp. 586–590.
- [6] O. A. Iupikov, M. V. Ivashina, and O. M. Smirnov, "Reducing the complexity of the beam calibration models of phased-array radio telescopes," in *Proc. EuCAP*, Apr. 2011, pp. 930–933.
- [7] B. D. Jeffs, K. F. Warnick, J. Landon, J. Waldron, D. Jones, J. R. Fisher, and R. Norrod, "Signal Processing for Phased Array Feeds in Radio Astronomical Telescopes," *Selected Topics in Signal Processing, IEEE Journal of*, vol. 2, no. 5, pp. 635–646, Oct. 2008.
- [8] M. Elmer, B. D. Jeffs, and K. F. Warnick, "Beamformer design methods for phased array feeds," in *International Workshop on Phased Array Antenna Systems for Radio Astronomy*, May 2010.
- [9] S. G. Hay, "SKA field of view de-rotation using connected array beam scanning with constant beam shape," in *Microwave Conference Proceedings (APMC), 2011 Asia-Pacific*, Dec. 2011, pp. 1174–1177.
- [10] S. J. Wijnholds, K. J. B. Grainge, and R. Nijboer, "Report on Calibration and Imaging Working Group Activities," Calibration and Imaging Working Group, Tech. Rep., 2012.
- [11] A. Young, R. Maaskant, M. V. Ivashina, and D. B. Davidson, "Performance Evaluation of Far Field Patterns for Radio Astronomy Application through the Use of the Jacobi-Bessel Series," in *Proc. Int. Conf. on Electromagn. in Adv. Applicat. (ICEAA)*, Cape Town, Sep. 2012.
- [12] V. Galindo-Israel and R. Mittra, "A new series representation for the radiation integral with application to reflector antennas," *IEEE Trans. Antennas Propag.*, vol. 25, no. 5, pp. 631–641, Sep. 1977.
- [13] Y. Rahmat-Samii and V. Galindo-Israel, "Shaped reflector antenna analysis using the Jacobi-Bessel series," *IEEE Trans. Antennas Propag.*, vol. 28, no. 4, pp. 425–435, Jul. 1980.
- [14] M. V. Ivashina and C. G. M. van't Klooster, "Focal fields in reflector antennas and associated array feed synthesis for high efficiency multi-beam performances," in *ESTEC Antenna Workshop*, 2002.
- [15] I. Theron, R. Lehmensiek, and D. de Villiers, "The design of the MeerKAT dish optics," in *Electromagnetics in Advanced Applications (ICEAA), 2012 International Conference on*, Sep. 2012, pp. 539–542.
- [16] R. C. Hansen, "A One-Parameter Circular Aperture Distribution with Narrow Beamwidth and Low Sidelobes," *IEEE Trans. Antennas Propag.*, pp. 477–480, Jul. 1976.
- [17] J. Ruze, "Lateral-feed displacement in a paraboloid," *IEEE Trans. Antennas Propag.*, vol. 13, no. 5, pp. 660–665, Sep. 1965.

- [18] W. A. Imbriale, P. G. Ingerson, and W. C. Wong, "Large Lateral Feed Displacements in a Parabolic Reflector," *IEEE Trans. Antennas Propag.*, vol. 22, no. 6, pp. 742–745, Nov. 1974.
- [19] Y. Y. Hu, "A method of determining phase centers and its application to electromagnetic horns," J. Franklin Inst., Tech. Rep., Jan. 1966.
- [20] O. I. Frost, "An algorithm for linearly constrained adaptive array processing," *Proc. IEEE*, vol. 60, no. 8, pp. 926–935, Aug. 1972.
- [21] H. L. van Trees, *Optimum Array Processing*. New York, N.Y.: Wiley, 2002.
- [22] M. V. Ivashina, O. A. Iupikov, R. Maaskant, W. A. van Cappellen, and T. Oosterloo, "An Optimal Beamforming Strategy for Wide-Field Surveys With Phased-Array-Fed Reflector Antennas," *IEEE Trans. Antennas Propag.*, vol. 59, no. 6, pp. 1864–1875, Jun. 2011.
- [23] P. G. Smith, "Measurement of the Complete Far-Field Pattern of Large Antennas by Radio-Star Sources," *IEEE Trans. Antennas Propag.*, vol. 14, no. 1, pp. 6–16, Jan. 1966.
- [24] W. van Cappellen, S. Wijnholds, and L. Bakker, "Experimental evaluation of polarimetric beamformers for an L-band phased array feed," in *Antennas and Propagation (EUCAP), 2012 6th European Conference on*, 2012, pp. 634–637.
- [25] S. J. Wijnholds, "Calculating Beam Pattern Inaccuracies and their Implications," in *3GC-II Workshop*, Albufeira (Portugal), Sep. 2011.
- [26] O. M. Smirnov and M. V. Ivashina, "Element gain drifts as an imaging dynamic range limitation in PAF-based interferometers," in *XXXth URSI General Assembly and Scientific Symposium*, Aug. 2011, pp. 1–4.
- [27] Harp, G. R. *et al.*, "Primary Beam and Dish Surface Characterization at the Allen Telescope Array by Radio Holography," *IEEE Trans. Antennas Propag.*, vol. 59, no. 6, pp. 2004–2021, Jun. 2011.



**Marianna V. Ivashina** Dr. Marianna V. Ivashina received a Ph.D. in Electrical Engineering from the Sevastopol National Technical University (SNTU), Ukraine, in 2001. From 2001 to 2004 she was a Postdoctoral Researcher and from 2004 till 2010 an Antenna System Scientist at The Netherlands Institute for Radio Astronomy (ASTRON). During this period, she carried out research on an innovative Phased Array Feed (PAF) technology for a new-generation radio telescope, known as the Square Kilometer Array (SKA). The results of these early projects have led to the definition of APERTIF - a PAF system that is being developed at ASTRON to replace the current horn feeds in the Westerbork Synthesis Radio Telescope (WSRT). Dr. Ivashina was involved in the development of APERTIF during 2008–2010 and acted as an external reviewer at the Preliminary Design Review of the Australian SKA Pathfinder (ASKAP) in 2009. She was a Guest Editor of the special issue of the *IEEE Transactions on Antennas and Propagation* for the Next Generation Radio Telescopes (June, 2011); and since 2011 she assists the SKA office in the development of the statement of work of the next phase of the SKA project. Dr. Ivashina has received several scientific distinctions including the 2nd Best Paper Award ('Best team contribution') at the ESA Antenna Workshop (2008) and the International Qualification Fellowship of the VINNOVA - Marie Curie Actions Program (2009). She is currently Associate Professor at the Antenna Group of the Signals and Systems Department (Chalmers University of Technology, Sweden). Her interests are phased arrays and reflector antennas, antenna system modeling techniques, array signal processing and radio astronomy.



**Rob Maaskant** (M'11) was born in the Netherlands on April, 14th, 1978. He received his M.Sc. degree (*cum laude*) in 2003, and his Ph.D. degree (*cum laude*) in 2010, both in Electrical Engineering from the Eindhoven University of Technology, Eindhoven, The Netherlands. His Ph.D. has been awarded "the best dissertation of the Electrical Engineering Department, 2010." From 2003–2010, he was employed as an antenna research scientist at the Netherlands Institute for Radio Astronomy (ASTRON), Dwingeloo, The Netherlands, and from 2010–2012 as a postdoctoral researcher in the Antenna Group of the Signals and Systems Department at the Chalmers University of Technology, Sweden, for which he won a Rubicon postdoctoral fellowship from the Netherlands Organization for Scientific Research (NWO), 2010. He is currently an Assistant Professor in the same Antenna Group. He is the primary author of the CAESAR software; an advanced integral-equation based solver for the analysis of large antenna array systems. His current research interest is in the field of receiving antennas for low-noise applications, meta-material based waveguides, and computational electromagnetics to solve these types of problems.

Dr. Maaskant received the 2nd best paper prize ('best team contribution') at the 2008 ESA/ESTEC workshop, Noordwijk, and was awarded a Young Researcher grant from the Swedish Research Council (VR), in 2011.



**André Young** was born in the Free State, South Africa on April 6, 1983. He received the B.Eng. degree in electrical and electronic engineering with computer science (*cum laude*) and M.Sc.Eng. degree in electronic engineering (*cum laude*) in 2005 and 2007, respectively, from the University of Stellenbosch, Stellenbosch, South Africa. His master's thesis was on mesh termination schemes for the finite element method in electromagnetics.

He has worked on various engineering projects for Azoteq (Paarl, South Africa) and Entersekt (Stellenbosch, South Africa), and is currently pursuing the Ph.D. degree in electronic engineering at the University of Stellenbosch, where he was also appointed as a Junior Lecturer in 2009 and 2011. Since 2011 he has spent several months as a visiting researcher with the Antenna Group at the Chalmers University of Technology, Gothenburg, Sweden. His main research interests include computational electromagnetics and antennas.



**Oleg Iupikov** Oleg Iupikov received a MSc degree (*cum laude*) in Electrical Engineering in 2006, from the Sevastopol National Technical University, Ukraine. After graduating till 2010, he was working at the Radio Engineering Bureau, Sevastopol. During this period, he was also a visiting scientist at The Netherlands Institute for Radio Astronomy (ASTRON), where he was involved in the development of the focal plane array simulation software for the APERTIF telescope. This visit was funded by the SKADS Marie Curie visitor grant and APERTIF project. From November 2011, he is a Ph.D. student at the Antenna Group of Chalmers University of Technology. His Ph.D. project is devoted to the development of numerical methods for optimization of focal plane array systems and their efficient calibration in the context of the next generation radio telescope known as the Square Kilometer Array (SKA).



**David Davidson** David Bruce Davidson (M'85-S'07-F'12) was born in London, U.K., 1961. He was raised and educated in South Africa, receiving the B.Eng, B.Eng (Hons), and M.Eng degrees (all cum laude) from the University of Pretoria, South Africa, in 1982, 1983, and 1986 respectively, and the Ph.D. degree from the University of Stellenbosch, Stellenbosch, South Africa, in 1991.

Following national service (1984-5) in the then South African Defence Force, he was with the Council for Scientific and Industrial Research, Pretoria, South Africa, prior to joining the University of Stellenbosch in 1988. As of 2011, he holds the South African Research Chair in Electromagnetic Systems and EMI Mitigation for SKA there. He was a Visiting Scholar at the University of Arizona in 1993, a Visiting Fellow Commoner at Trinity College, Cambridge University, England in 1997, a Guest Professor at the IRCTR, Delft University of Technology, The Netherlands, in 2003, and an Honorary Visitor, University of Manchester, UK in 2009. His main research interest through most of his career has been computational electromagnetics (CEM), and he has published extensively on this topic. He is the author of the recently revised text "Computational Electromagnetics for RF and Microwave Engineering" (Cambridge, U.K.: Cambridge Univ. Press, 1st edn, 2005, 2nd edn, 2011). Recently, his interests have expanded to include engineering electromagnetics for radio astronomy.

Prof. Davidson is a member of the South African Institute of Electrical Engineers and the Applied Computational Electromagnetic Society. He is a recipient of the South African FRD (now NRF) President's Award; presently, he has a B2 research rating from the NRF. He received the Rector's Award for Excellent Research from the University of Stellenbosch in 2005. He is a Past Chairman of the IEEE AP/MTT Chapter of South Africa, and served as an Associate Editor of the IEEE Antennas And Wireless Propagation Letters ('06-08). Currently, he is the editor of the "EM Programmer's Notebook" column of the IEEE Antennas And Propagation Magazine, and is serving on the IEEE Antennas and Propagation AdCom ('11-'13). He served as General Chair of the "8th International Workshop on Finite Elements for Microwave Engineering", held in Stellenbosch, May 2006. He was Chair of the local organizing committee of ICEAA-IEEE APWC-EEIS'12, held in Cape Town in September 2012.